Thermal conductivity of bulk boron nitride nanotube sheets and their epoxy-impregnated composites

Jakubinek, Michael B.; Niven, John F.; Johnson, Michel B.; Ashrafi, Benham; Kim, Keun Su; Simard, Benoit; White, Mary Anne

Publisher's version / Version de l'éditeur:
https://doi.org/10.1002/pssa.201533010
Physica Status Solidi (A) Applications and Materials, 213, 8, pp. 2237-2242, 2016-03-10

NRC Publications Record / Notice d'Archives des publications de CNRC:
https://nrc-publications.canada.ca/eng/view/object/?id=01e4ef00-e2d0-4de6-aa56-efc8eba12c43
https://publications-cnrc.canada.ca/fra/voir/objet/?id=01e4ef00-e2d0-4de6-aa56-efc8eba12c43

Thermal conductivity of bulk boron nitride nanotube sheets and their epoxy-impregnated composites

Michael B. Jakubinek[*,1], John F. Niven[2], Michel B. Johnson[3], Behnam Ashrafi[4], Keun Su Kim[1], Benoit Simard[,1] and Mary Anne White[2,3,5]**

[1] Security and Disruptive Technologies, Division of Emerging Technologies, National Research Council Canada, Ottawa, ON K1A 0R6, Canada
[2] Department of Physics and Atmospheric Science, Dalhousie University, Halifax, NS B3H 4R2, Canada
[3] Institute for Research in Materials, Dalhousie University, Halifax, NS B3H 4R2, Canada
[4] Aerospace, Division of Engineering, National Research Council Canada, Montreal, QC H3S 2B2, Canada
[5] Department of Chemistry, Dalhousie University, Halifax, NS B3H 4R2, Canada

Received ZZZ, revised ZZZ, accepted ZZZ
Published online ZZZ (Dates will be provided by the publisher.)

Keywords boron nitride nanotubes, buckypaper, nanocomposites, thermal conductivity.

* Corresponding author: e-mail Michael.Jakubinek@nrc-cnrc.gc.ca, Phone: +1 613 990 4250
** Corresponding author: e-mail Benoit.Simard@nrc-cnrc.gc.ca, Phone: +1 613 990 0977

The thermal conductivity of bulk, self-supporting boron nitride nanotube (BNNT) sheets composed of nominally 100% BNNTs oriented randomly in-plane was measured by a steady-state, parallel thermal conductance method. The sheets were either collected directly during synthesis or produced by dispersion and filtration. Differences between the effective thermal conductivities of filtration-produced BNNT buckypaper (~1.5 W m^{-1} K^{-1}) and lower-density as-synthesized sheets (~0.75 W m^{-1} K^{-1}), which are both porous materials, were primarily due to their density. The measured results indicate similar thermal conductivity, in the range of 7 to 12 W m^{-1} K^{-1}, for the BNNT network in these sheets. High BNNT-content composites (~30 wt.% BNNTs) produced by epoxy impregnation of the porous BNNT network gave 2 to 3 W m^{-1} K^{-1}, more than 10× the baseline epoxy. The combination of manufacturability, thermal conductivity, and electrical insulation offers exciting potential for electrically insulating, thermally conductive coatings and packaging.

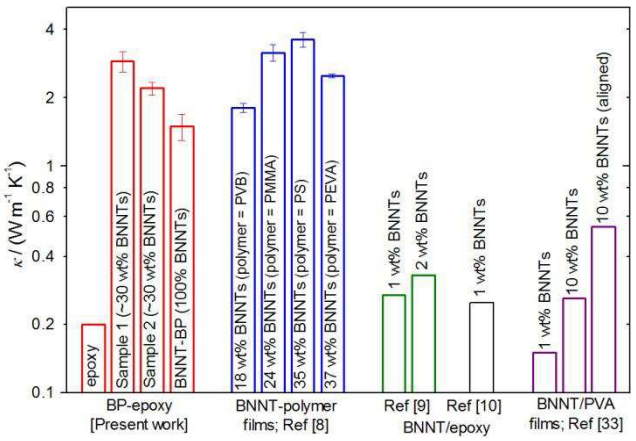

Thermal conductivity of free-standing BNNT buckypaper, buckyaper composites, and related materials at room temperature

1 Introduction Boron nitride nanotubes (BNNTs) are structurally analogous to carbon nanotubes (CNTs) and share some similarly exceptional properties, including high strength and stiffness, low density, and good thermal conductivity, but also offer a different set of multifunctional advantages that include electrical insulation, higher temperature stability, piezoelectricity and high neutron absorption [1,2]. BNNTs, while first reported soon after CNTs [3], have received far less attention due to more challenging synthesis and consequently limited supply. Recent works [4,5] are addressing this limitation and, with the availability of new commercial BNNTs [6,7], there are increased

opportunities to study and exploit the properties of BNNTs. The combination of electrical insulation and thermal conductivity is one case where BNNTs offer a clear advantage for application to thermal interface materials and electrically insulating substrates/ packaging materials [8-10] or heat transfer fluids [11].

The thermal conductivity (κ) of individual, high-quality CNTs is known to be high (> 3000 W m^{-1} K^{-1} at 300 K [12]), and has now been studied with a variety of CNT samples and measurement methods [13]. In contrast, there are few experimental measurements for BNNTs. A through-thickness thermal conductivity of 0.96 W m^{-1} K^{-1} was reported for a pellet of BNNTs compressed under pressure [14], and a comparable value (~ 2 W m^{-1} K^{-1})measured on BNNT bundles led to a prediction of high κ_{BNNT} [15]. A value of ~325 W m^{-1} K^{-1} measured on isotopically enriched ^{11}B multi-walled BNNTs was equal to that of similar diameter CNTs, while a natural abundance ($^{10}B/^{11}B$) BNNT gave ~ 200 W m^{-1} K^{-1} [16]. This result is consistent with a reduction in the phonon mean free path due to isotope scattering. Based on a higher specific heat capacity for BNNT it was suggested that BNNTs could have higher κ than CNTs [17], which could be realized in isotopically pure BNNTs. In any case, the experimental work to date shows that BNNTs, like CNTs, are good thermal conductors. Therefore, for BNNT-filled composites or macroscopic BNNT assemblies (*e.g.*, yarns, sheets, films, arrays) κ could be expected to be similar to related CNT materials, which cover a wide range from high values comparable to metals to aerogel-like, low values [13,18]. For paper-thick, non-woven sheets of CNTs, often called buckypaper, the measured thermal conductivities are generally modest and in the range of 1 to 10 W m^{-1} K^{-1} at room temperature [18]. This is attributed to factors including nanotube quality, bundling, and tube-tube contact resistance [18]. Simulations have shown the combination of CNT length and κ_{CNT} can explain a wide range of measured values for buckypaper sheets [19].

There are only a few reports of BNNT assemblies including films and arrays composed of nominally 100% BNNTs (*e.g.*, refs [20-22]) and, aside from BNNT bundles [15], thermal conductivity of free-standing BNNT assemblies has not been reported in the literature. Here we report the thermal conductivity of BNNT sheets deposited directly during synthesis, denoted as "as-synthesized" (AS) sheets, and of higher-density BNNT "buckypaper" (BP) sheets produced by vacuum filtration, as well as polymer composites produced by epoxy-impregnation of preformed buckypaper. The thermal conductivities, the first reported for large-scale BNNT assemblies, are comparable to those reported for CNT buckypapers despite the possibility of lower κ of BNNTs produced from non-isotopically enriched boron. While lower than reports for higher-density, aligned CNT assemblies [23-26] and metals, the thermal conductivities are at least 10× higher than typical insulating polymers. Nanotube sheets also offer advantages in terms of form factor, manufacturability and integration into composites. These features, along with the present thermal conductivity results, indicate the potential of BNNT buckypapers for applications as an electronic packaging material or heat-dissipating substrates.

2 Experimental Methods BNNTs were synthesized from hexagonal boron nitride powder (hBN, MK-hBN-N70 from MK Impex Corp) fed into a Tekna PS-50 induction plasma torch (Tekna Plasma Systems Inc.). As described elsewhere in greater detail [4], hydrogen is incorporated into the process gas mixture (Ar, N_2, H_2) and its presence results in formation of B-N-H intermediate species that provide a more efficient source of nitrogen than a direct N_2 + B reaction. The features of the process (*i.e.*, high temperature, high cooling rate and gas composition) led to the growth of small diameter (~ 5 nm), highly crystalline BNNTs at high yield (> 20 g h^{-1}) [4]. Several morphologies (sheets, fibrous, aerogel) deposit in the reactor and as-synthesized BNNT sheets (AS sheets, Figure 1a,d) were collected directly. A continuous layer with no obvious delamination was peeled off and cut into strips for characterization. SEM imaging (Figure 1d) shows a low-density network consisting primarily of high-aspect ratio particles along with impurities, which include amorphous boron and hBN [4]. The purity of the as-synthesized material is estimated to be over 50% BNNTs based on thermogravimetric analysis and imaging and the density of the AS sheets was approximately 0.15 g cm^{-3}. Higher-density BNNT buckypapers (BP sheets, Figure 1b,e) of approximately 0.3 g cm^{-3} were produced from solvent dispersions of purified BNNTs by vacuum filtration. Purification consisted of a series of thermal and solvent treatments prior to production of the BP sheet [4,27]. These BNNT BP sheets wet readily with low viscosity epoxy resin, which enabled production of high-loading BNNT BP-epoxy composites [27]. This approach, involving wetting the BP sheet with pre-heated epoxy resin/hardener (Araldite MY0510 epoxy with 4-4' DDS hardener at the recommended mixing ratio of 49 parts per hundred resin) followed by curing at elevated temperature under compression, was employed to produce a BNNT BP-epoxy composite sheet containing ~30 wt.% BNNTs oriented randomly in the plane of the sample (Figure 1c,f).

Thermal conductivities of the BNNT sheets were measured using the parallel thermal conductance (PTC) method [28], which has been applied previously to characterize CNT sheets and yarns [23,24,29]. This steady-state method is ideal for nanotube sheet samples because they cannot support thermometers or heaters as required by some conventional methods. A low-κ support carries heat in parallel to the sample and the background thermal conductance is accurately measured and subtracted. BNNT sheets were cut into $3\times12\times t$ mm^3 strips, where t is the thickness, and attached to the measurement platform using silver paint (DuPont 4929 N).

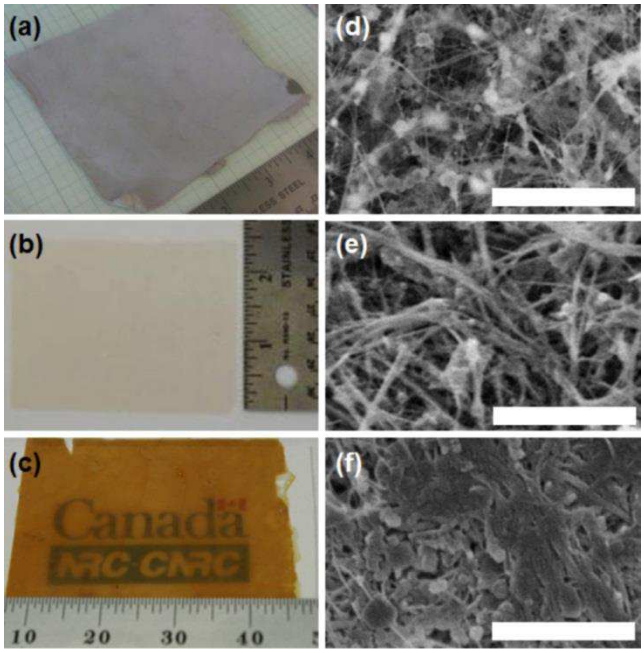

Figure 1. BNNT sheet materials. (a) AS sheet collected directly from the synthesis; (b) BP sheet produced by vacuum filtration; (c) BP-epoxy sheet; and (d-f) SEM images of the AS, BP, and BP-epoxy sheets, respectively (scale bars = 1 μm).

The custom measurement platform (Figure 2a) was mounted on a standard resistivity measurement puck of a physical properties measurement system (PPMS, Quantum Design), which simplified connection of the heater and thermocouple within the cryogenic and vacuum chamber of the PPMS. The accuracy of this PTC measurement platform has been verified against known materials including alumel and nichrome (κ accurate within 10%) and Pyrex® (κ accurate within 5%). The thickness of the BNNT sheet materials was determined by optical microscopy at several points along the sample (e.g., Figure 2b). Measurements of thermal conductance were performed under vacuum ($<10^{-4}$ Torr) within the temperature range 50 K to 325 K. Three measurements (Figure 2a) are required to calculate thermal conductance for each sample: a total thermal conductance measurement, a radiation measurement, and a background measurement [28]. The sample conductance is typically a small contribution, ~20% of the background at 300 K.

3 Results & Discussion The thermal conductivities for AS and BP sheets from 50 to 325 K are shown in Figure 3. The sheets show similar temperature dependence to each other, and to CNT assemblies [23,24], but with higher κ for the higher density BP sheets. The major contribution to uncertainty comes from the sample thicknesses. In particular, the greater variability observed in the results for the AS sheets is attributed to higher uncertainty in their thickness and hence density, which was estimated from the mass and dimensions of a 10 cm x 10 cm AS sheet, as the thickness of these sheets varies more than for filtration-produced BP sheets. For comparison between the two sheet types and literature results for other nanotube materials, it is important to note the measured thicknesses are for porous materials where the densities differ and in both cases are significantly lower than the density of an individual BNNT. Therefore, the results obtained are *effective* thermal conductivities determined by both the BNNT network and the porosity of the sheets and only a fraction of the cross-sectional area of the sheet is actually contributing to heat conduction. The thermal conductivity of the BNNT network can be estimated by considering this measured κ and the ratio of the density of hBN (2.1 g cm^{-3}) to the density of the bulk BNNT sheets determined from their mass and external dimensions. Table 1 summarizes the thermal conductivities for multiple samples of each sheet and, when scaled by this density ratio, the AS sheets (~ 7 to 11 W m^{-1} K^{-1} on average) and BP sheets (~ 9 to 12 W m^{-1} K^{-1} on average) fall in a similar range in terms of the thermal conductivity of the BNNT networks. The BNNT sheets still show much lower κ than individual BNNTs [15], but the values compare well with previous measurements of related BNNT [15] and CNT materials [18].

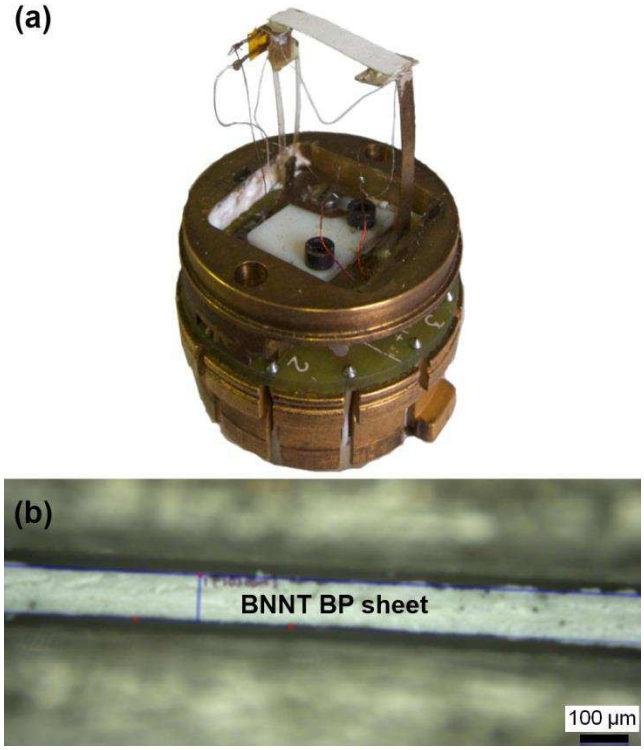

Figure 2. (a) BNNT BP sheet mounted across the PTC sample stage (radiation shield cap not shown). The long, narrow supports for the hot platform, which supports a resistance heater and one end of the sample are designed to minimize background thermal conductance. (b) Measurement of BNNT sheet thickness by optical microscopy (cross-sectional view).

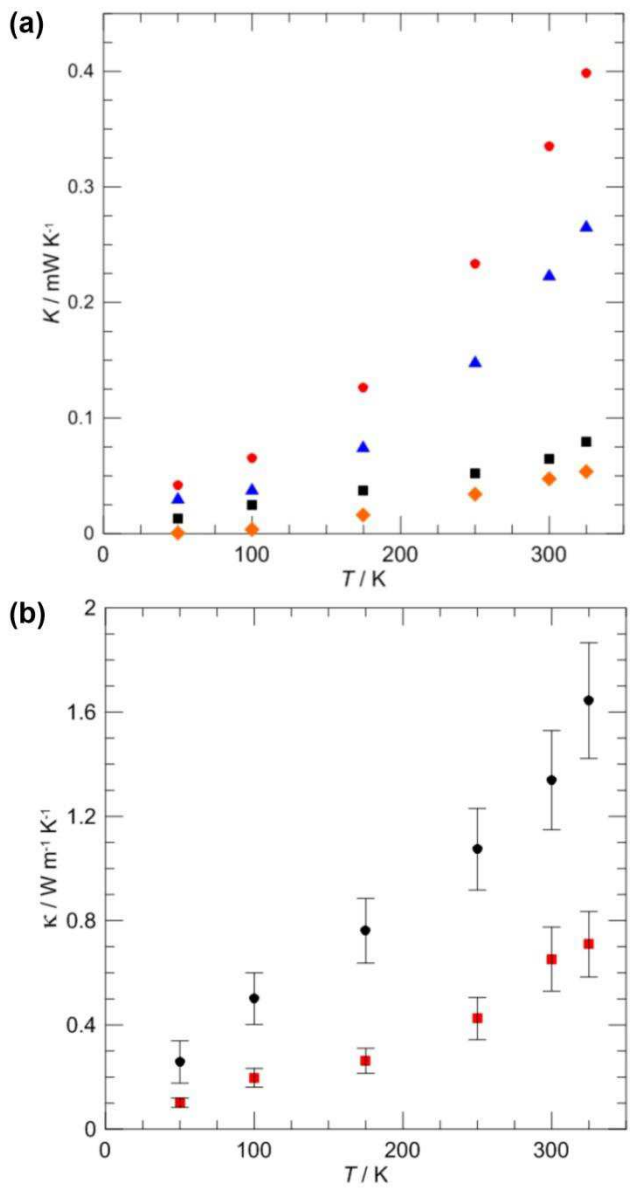

Figure 3. (a) Contributions to the thermal conductance, K, for BNNT BP, where K_{tot} (●), K_{back} (▲), K_{sample} (■), and K_{rad} (♦) are, respectively, the conductance due to the total assembly, the background, the sample, and radiation. (b) κ as a function of temperature of a AS (■) and BP (●) BNNT sheets.

The similarity of the scaled results indicates that the thermal conductivity of the BNNT network is similar in both the AS and BP sheets. The individual BNNT thermal conductivity, κ_{BNNT}, is expected to be similar in both cases, as the BNNTs came from the same production process, and the higher average value for the BP sheet is likely influenced by its higher purity. The BP sheets were produced from a purified BNNT sample. However, the thermal conductivity of nanotube networks is also known to be reduced by tube-tube contact resistance, bundling and misalignment [18], and the relative merits of BP compared to AS sheets in this regard are less obvious. For example the SEM imaging (Figure 1) indicates smaller bundle sizes in the AS sheet and dispersion steps involving sonication required to produce the BP sheet can shorten nanotubes, both of which are known to reduce thermal conductivity of analagous CNT sheets [18].

Table 1. κ of BNNT sheet samples measured at T = 300K and $\kappa_{BNNT\ network}$, the thermal conductivity of the BNNT network.

Sample	κ (W m^{-1} K^{-1})	$\kappa_{BNNT\ network}$* (W m^{-1} K^{-1})
AS Sheet 1a	0.50 ± 0.04	7.0 ± 1.5
b	0.80 ± 0.11	11.2 ± 3.0
c	0.65 ± 0.12	9.1 ± 2.9
AS Sheet 2a	0.49 ± 0.05	6.7 ± 1.5
b	0.72 ± 0.07	10.1 ± 2.3
c	0.52 ± 0.04	7.3 ± 1.5
BP sheet 1a	1.67 ± 0.31	11.7 ± 2.8
b	1.49 ± 0.23	10.4 ± 2.1
BP sheet 2a	1.34 ± 0.19	9.4 ± 1.8
b	1.41 ± 0.19	9.9 ± 1.8
c	1.59 ± 0.22	11.1 ± 2.1

*Scaled result considering the ratio of the apparent cross-sectional area of the macroscopic sample and the area involved in heat conduction. Scaling is a simple multiplication by the ratio of the density of hBN (2.1 g/cc) to the average density of the sheets, which assumes all heat is carried by the nanotube network.

While much lower than for individual BNNTs, the present thermal conductivity values are much higher than achieved with typical polymers (~0.15 to 0.3 W m^{-1} K^{-1}) and also higher than nanotube-polymer composites with dispersed nanotubes [18,30]. The combination of the modest thermal conductivity of BNNT sheets with their very high electrical resistivity and thermal stability, as well as high dielectric constant and breakdown strength, offers a potentially advantageous set of properties for electronics packaging materials or substrates. As a representative of such a composite, an epoxy-impregnated BNNT buckypaper also was characterized using the PTC thermal conductivity measurement method at room temperature. Figure 4 reports the thermal conductivity of similar pristine and epoxy-impregnated BP sheets, along with comparison to literature reports. Two samples were measured, to assess both measurement uncertainty and variation attributable to the sample preparation; the results were values of 2.9 ± 0.3 W m^{-1} K^{-1} and 2.2 ± 0.15 W m^{-1} K^{-1}. These BP-epoxy composites contain ~ 30 wt% BNNTs based on the change in mass after impregnation and thermogravimetric analysis in air; the latter yields the residual mass of BNNTs left after oxidation of the polymer. The measured thermal conductivity is larger than that for the dry BP sheet, but lower than that for the BNNT network and compares well with a

rule of mixtures estimate considering the BP-epoxy sample as a composite consisting of 30% BNNT network and 70% epoxy. As illustrated graphically, the thermal conductivity of the epoxy impregnated sheets is more than 10 times that of the neat epoxy (0.2 W m^{-1} K^{-1}). The thermal conductivity of BNNT buckypaper has not been previously reported but this level of increase relative to epoxy is similar to a previous report by Zhi *et al.* [8], where supported BNNT mats were infiltrated with a series of polymers (PVB, PS, PMMA, PEVA) to achieve 18 to 37 wt% BNNTs and measured thermal conductivities of 1.8 to 3.6 W m^{-1} K^{-1}. Similarly prepared BN nanoplatlet composites were reported to have lower thermal conductivity (under 1.5 W m^{-1} K^{-1}) at 30 wt% BN, but values as high as 5.2 W m^{-1} K^{-1} were reported with BN content of 70 wt% [31].

These report and the present work show significantly higher values than reported for BNNTs dispersed into a polymer matrix [9,10,32,33]. The improved breakdown strength and reduced coefficient of thermal expansion, also reported by Zhi *et al.* [8], illustrates additional multifunctional improvements obtained with electrically insulating, thermally conductive BNNT-polymer composites.

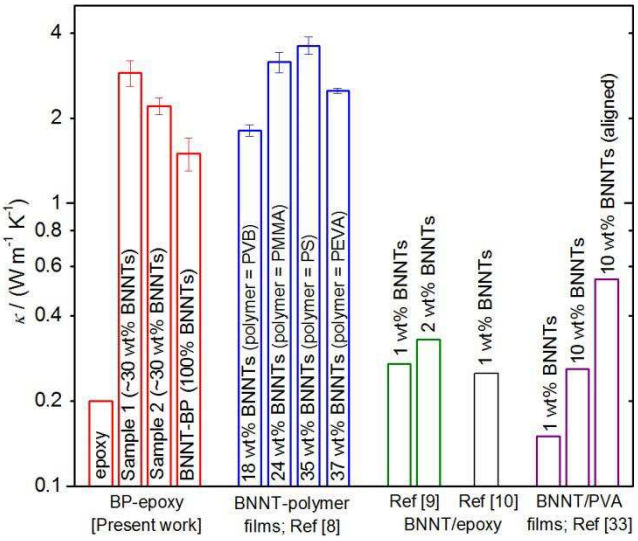

Figure 4. Room-temperature κ values of the epoxy-impregnated BNNT buckypaper sheets and related materials ([8-10, 33]).

4 Conclusions In summary, we report the first direct thermal conductivity measurements for bulk BNNT sheets composed of nominally 100 wt% BNNTs, as well as the thermal conductivity of epoxy-impregnated BNNT buckypaper composites. For pure BNNT sheets, κ varied from 0.5 to 0.8 W m^{-1} K^{-1} for as-synthesized sheets, and from 1.3 to 1.7 W m^{-1} K^{-1} for filtration-produced buckypaper sheets. The difference between the two cases can be attributed in large part to the difference in density, as in both cases the thermal conductivity of the BNNT network is estimated to be similar and in the range of 7 – 12 W m^{-1} K^{-1}. The higher average value for the BNNT network in the BP sheet could be attributed to higher BNNT purity, as these sheets were produced from purified BNNTs, and differences in the network morphology (*e.g.*, bundle size, contacts, alignment), although it is not obvious the latter are more favourable for the BP sheet. While the thermal conductivities are much lower than for individual BNNTs, the results for both pure and epoxy-impregnated BNNT sheets are much higher than for insulating polymers. The measured room-temperature thermal conductivity for the high BNNT-content composites (~30 wt% BNNTs) is improved 10-fold relative to the epoxy. The combination of the manufacturability of BNNT buckypaper with its thermal conductivity, electrical insulation, and other functional properties of BNNTs offers exciting potential for electrically insulating, thermally conductive coatings and packaging. This work also provides a first determination of the thermal conductivity of free-standing BNNT sheets produced at the bulk scale and we anticipate that further development of macroscopic BNNT assemblies, including improved purification, increased density and aligned versions (sheets and fibers), will lead to high thermal conductivity values as seen for comparable CNT materials.

Acknowledgements The authors thank Mark Plunkett and Amy Hrdina for supporting synthesis and purification of the BNNT materials, Gordon Chan for SEM, and acknowledge support for development of BNNT materials from the NRC-Security Materials Technology Program. Thermal conductivity measurements were supported by NSERC and the Canada Foundation for Innovation, Atlantic Innovation Fund and other partners that fund the Facilities for Materials Characterization managed by the Institute for Research in Materials at Dalhousie University.

References

[1] W. Meng, Y. Huang, Y. Fu, Z. Wang, C. Zhi. J Mater Chem C **2**, 10049 (2014).
[2] J. Hurst in *Nanotube Superfiber Materials*, *Ed.* M.J. Schulz, V.N. Shanov, Z. Yin, William Andrew, 2014, pp. 267-287.
[3] N. Chopra, R. Luyken, K. Cherrey, V. Crespi, M. Cohen, S. Louie, and A. Zettl. Science **269** 5226 (1995), p. 966.
[4] K.S. Kim, C.T. Kingston, A. Hrdina, M.B. Jakubinek, J. Guan, M. Plunkett, B. Simard. ACS Nano **8**, 6211 (2014).
[5] A. Fathalizadeh, T. Pham, W. Mickelson, A. Zettl. Nano Lett 14, 4881, 2014.
[6] BNNT, LLC. www.bnnt.com/news/24-better-nanotubes
[7] Tekna http://tekna.com/tekna-launches-a-revolutionary-material-on-the-market-boron-nitride-nanotubes/
[8] C. Zhi, Y. Bando, T. Terao, C. Tang, H. Kuwaraha, D. Golberg. Advanced Functional Materials **19**, 1857 (2009).
[9] J. Su, Y. Xiao, M. Ren. Phys Stat Sol A **210**, 2699 (2013).
[10] H. Yan, Y. Tang, J. Su, X. Yang, Appl Phys A **114**, 331 (2014)
[11] C. Zhi, Y. Xu, Y. Bando, D. Golberg. ACS Nano **5**, 6571 (2011).
[12] P. Kim, L. Shi, A. Majumdar, and P. L. McEuen. Phys Rev Lett **87**, 215502 (2001).

[13] A.M. Marconnet, M.A. Panzer, K.E. Goodson. Rev Mod Phys **85**, 1295 (2013).
[14] C. Tang, Y. Bando, C. Liu, S. Fan, J. Zhang, X. Ding, D. Golberg. J Phys Chem B **110**, 10354 (2006).
[15] C.W. Chang, W.-Q. Han, A. Zettl. Appl Phys Lett **86**, 173102 (2005).
[16] C.W. Chang, A.M. Mennimore, A. Afanasiev, *et al*. Phys Rev Lett **97**, 085901 (2006).
[17] Y. Xiao, X.H. Yan, J. Xiang, Y.L. Mao, Y. Zhang, J.X. Cao, J.W. Ding. Appl Phys Lett **84**, 4626 (2004).
[18] M.B. Jakubinek. in *Nanotube Superfiber Materials*, *Ed*. M.J. Schulz, V.N. Shanov, Z. Yin, William Andrew, 2014, pp. 425-456.
[19] A.N. Volkov, L.V. Zhigilei. Appl Phys Lett **101**, 043113 (2012).
[20] L.H. Li, Y. Chen. Langmuir **26**, 5135 (2010).
[21] L.H. Li, Y. Chen, A.M. Glushenkov. J Mater Chem **20**, 9679 (2010).
[22] Y. Wang, Y. Yamamoto, H. Kiyono, S. Shimada. J Nanomaterials, **2008**, 606283 (2008).
[23] M. B. Jakubinek, M. B. Johnson, M. A. White *et al*. Carbon, **50**, 244 (2012).
[24] J. H. Pohls, M. B. Johnson, M. A. White, *et al*. Carbon, **50**, 4175 (2012).
[25] L. Zhang, G. Zhang, C. Liu, S. Fan. Nano Lett, **12**, 4848 (2012).
[26] N. Behabtu, C.C. Young, D.E. Tsentalovich, et al. Science **339** 6116, 182 (2013).
[27] K.S. Kim, M.B Jakubinek, Y. Martinez-Rubi, et al. RSC Adv, 5, 41186 (2015).
[28] B.M. Zawiliski, R.T. Littleton IV, and T.M. Tritt, Rev. Sci. Instrum., **72**, 1770 (2001).
[29] M.B. Jakubinek, B. Ashrafi, J. Guan, M.B. Johnson, M.A. White, B. Simard. RSC Advances 4, 57564 (2014).
[30] Z. Han, A. Fina, Progress in Polymer Science **36**, 914 (2011).
[31] Z. Wang, Y. Fu, W. Meng, C. Zhi. Nano Res Lett **9**, 643 (2014).
[32] T. Terao, Y. Bando, M. Mitome, C. Zhi, C. Tang, D. Golberg. J Phys Chem C 113, 13605 (2009).
[33] T. Terao, C. Zhi, Y. Bando, M. Mitome, C. Tang, D. Golberg. J Phys Chem C 114, 4340 (2010).